The Journal of Infectious Diseases

BRIEF REPORT

Pertussis Toxin Promotes Pulmonary Hypertension in an Infant Mouse Model of *Bordetella pertussis* Infection

Karen M. Scanlon,[1] Ling Chen,[2] and Nicholas H. Carbonetti[1]

[1]Department of Microbiology and Immunology, University of Maryland School of Medicine, Baltimore, Maryland, USA, and [2]Department of Physiology and Medicine, University of Maryland School of Medicine, Baltimore, Maryland, USA

Pertussis, caused by *Bordetella pertussis*, is a reemerging disease that can produce severe disease manifestations in infants, including pulmonary hypertension (PH). *B. pertussis*-induced PH is a major risk factor for infection-induced death, but the molecular mechanisms promoting PH are unknown and there is no effective treatment. We examined *B. pertussis*-induced PH in infant and adult mouse models of pertussis by Fulton index, right heart catheterization, or Doppler echocardiogram. Our results demonstrate that *B. pertussis*-induced PH is age related and dependent on the expression of pertussis toxin by the bacterium. Hence, pertussis toxin-targeting treatments may ameliorate PH and fatal infant infection.

Keywords. *Bordetella pertussis;* pulmonary hypertension; pertussis toxin; infant.

Pertussis in infants is associated with severe disease manifestations, such as pulmonary hypertension (PH) and kills over 160 000 children annually [1]. While infant pertussis is associated with respiratory distress, lung consolidation, and difficult ventilation, these features do not correlate with severe outcomes [2, 3]. However, the onset of PH in *Bordetella pertussis*-infected infants is a major risk factor for infection-induced death [3]. PH-induced right heart failure, not caused by *B. pertussis*, is typically preceded by increased right ventricle (RV) filling pressures, elevated afterload, and decreased RV function. Hallmarks of RV adaptation to increased RV afterload include RV hypertrophy and increased RV contractility [4]. In humans, only echocardiogram descriptions of pertussis-associated PH features are defined. Infants with pertussis develop signs of acute cor pulmonale such as RV dysfunction and dilation, increased arterial pressure, and tricuspid regurgitation [5]. *B. pertussis*-induced PH can lead to cardiac ischemia, cardiac arrest, and cardiac failure even when treated with inhaled nitric oxide and/or extracorporeal membrane oxygenation [2, 6]. Despite an urgent need for an evidence base that might optimize the management of severe pertussis, the mechanism of *B. pertussis*-induced PH is unknown and appropriate treatment strategies for this severe disease have yet to be identified.

We have previously examined age-related responses to *B. pertussis* using infant (postnatal day 7, P7) and adult (6-week-old) mice [7]. With this approach, *B. pertussis*-induced lethality was found to be dependent on host age and bacterial expression of pertussis toxin (PT) [7]. *B. pertussis* disseminated from the lungs of infant mice and induced leukocytosis and elevated heart rate in a PT-dependent manner [7]. It is speculated that PT-mediated induction of leukocytosis causes vascular occlusions and promotes PH in pertussis but without a model system neither the role of PT in pertussis-associated PH nor the impact of potential therapeutics could be evaluated. In this study, we developed a model of *B. pertussis* infection-induced PH in infant mice and examined the role PT in the manifestation of pertussis-associated PH.

METHODS

Aerosol Inoculation

Infant P7 and adult 6- to 8-week-old male and female C57BL/6 mice were used in accordance with the University of Maryland, Baltimore Institutional Animal Care and Use Committee, and aerosol inoculated as previously described [7]. In brief, a Tohama I derivative of *B. pertussis* (wild type, WT) and an isogenic PT-deficient strain of *B. pertussis* (ΔPT) were grown on Bordet-Gengou agar plates for 48 hours and resuspended in phosphate-buffered saline (PBS). Bacterial suspensions or sham inoculum (PBS) were administered via a nebulizer system (Pari Vios) for 20 minutes.

Structural and Functional Assessment of the Right Ventricle

At 7 days postinoculation (dpi), the impact of infection on the heart was examined. Echocardiography was performed under anesthesia using a VisualSonics Vevo 2100 (VisualSonics) equipped with a 40 MHz array transducer. The sonographer (LC) who performed the imaging and calculations was blinded to animal groups. Open chest RV catheterization was also performed under anesthesia. In brief, mice were mechanically ventilated using a customized endotracheal tube, thoracotomy was performed, and a 1-Fr Mikro-tip catheter (SPR-1000, Millar Instruments) was inserted into the RV. After stabilization, RV pressure was recorded for a further 10 minutes (MP 100 with AcKnowledge version 3.7; BioPac Systems) for off-line analysis. For Fulton index measurements, the RV free wall, left ventricle (LV) and septum tissue were harvested and weighed and

Received 12 March 2021; editorial decision 14 June 2021; accepted 16 June 2021; published online June 19, 2021.

Correspondence: Karen M. Scanlon, PhD, Department of Microbiology and Immunology, University of Maryland School of Medicine, 685 West Baltimore, Baltimore, MD 21201 (kscanlon@som.umaryland.edu).

The Journal of Infectious Diseases® 2022;225:172–6

https://doi.org/10.1093/infdis/jiab325

the weight ratio of RV to LV plus septum was determined (see Supplementary Material for full description). Significance was determined by analysis of variance (ANOVA) using GraphPad Prism.

RESULTS

Bordetella pertussis Induces PT-Dependent Structural Changes in the Right Heart of Infant But Not Adult Mice

Earlier work by our group indicated that *B. pertussis* altered cardiac function in an infant mouse model of severe pertussis [7]. We have expanded on this observation by measuring the Fulton index, a correlate of PH which quantifies RV hypertrophy by measuring the relative weight of the RV free wall. At 7 dpi, a time point at which infected infant mice display dramatic leukocytosis and begin to lose weight [7], infant mice challenged with PT-expressing *B. pertussis* (WT) displayed significant RV hypertrophy (increased RV wall weight) compared with sham-inoculated mice (Figure 1). WT-infected infant mice displayed an average increase in Fulton index of 0.07, a value consistent with the manifestation of PH in mice [8] (see Supplementary Material for additional details). In keeping with the age-relatedness of pertussis-associated PH in humans, cardiac pathology as determined by Fulton index was not detected in WT-infected adult mice (Figure 1). An increase in Fulton index was not observed with ΔPT infection in either infant or adult mice. The PT-associated effect on RV structure in infants was further analyzed by echocardiography. At 7 dpi, infant mice infected with WT displayed significant increases in RV free wall thickness at end systole (RVWs) and end diastole (RVWd) that were not observed with ΔPT infection (Table 1). A measure of RV dilation was not achievable; however, the dimensions of the LV could be determined. Infant mice infected with WT, but not ΔPT, displayed a significant reduction in the LV dimension during diastole (LVDd; Supplementary Table 1). Because the heart displays diastolic ventricular interdependence [4], this result is indicative of an enlarged RV in animals infected with PT-expressing *B. pertussis*.

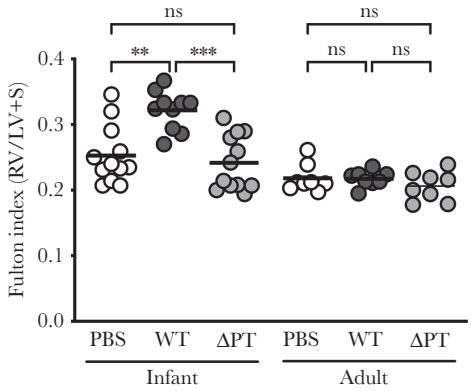

Figure 1. PT expressed during *B. pertussis* infection promotes RV hypertrophy in infant but not adult mice. At 7 dpi, infant mice inoculated at postnatal day 7 displayed significant RV hypertrophy in response to infection with PT-expressing *B. pertussis* (WT, dark gray circles) as determined by Fulton index. RV hypertrophy was not promoted by sham PBS inoculation (white circles), infection with a PT-deficient strain (ΔPT, light gray circles), or by infection with either strain in adult mice. Each circle represents an individual animal, bar represents the mean of the group. *P* values were determined by 1-way ANOVA with Tukey multiple comparison test; $^{**}P < .01$, $^{***}P < .001$. Data are representative of at least 2 independent experiments of n ≥ 4. Abbreviations: ANOVA, analysis of variance; dpi, days postinoculation; LV, left ventricle; ns, nonsignificant; PBS, phosphate-buffered saline; PT, pertussis toxin; RV, right ventricular; S, septum; WT, wild type.

PT-Expressing *B. pertussis* Increases Pressure and Promotes Inotropy in the Hearts of Infant Mice

Having detected a rapid, PT-dependent onset of RV remodeling in infant mice, we next explored how *B. pertussis* infection impacted cardiac function in these animals. By echocardiography, mean pulmonary arterial pressure (mPAP) was significantly increased in infant mice infected with WT but not ΔPT (Table 1). Consistent with this finding, RV outflow tract acceleration time, which has been shown to progressively shorten with increasing degrees of mPAP [9], was significantly decreased with WT infection (Table 1). Right heart catheterization is the gold standard for diagnosing PH. Given the small size of the RV in infant mice, it was not possible to measure volume changes; however, pressure measurements by open chest RV catheterization were recorded. At 7 dpi, RV end-systolic pressure (RVESP), a measure indicative of increased afterload, was significantly elevated in WT-infected infant mice and this increase was dependent on the expression of PT by the bacterium (Table 1). RV end-diastolic pressure (RVEDP), or filling pressure, was significantly increased by WT infection but not significantly increased in ΔPT-infected mice (Table 1). Because of the Anrep effect, abrupt increases in RV afterload can promote increased contractility. Maximum RV dP/dt, the instantaneous rate of RV pressure rise, is used as a surrogate marker for cardiac inotropy or RV contractility [10]. Infant mice infected with PT-expressing *B. pertussis* displayed significantly increased RV contractility (RV dP/dt max) compared with both sham-inoculated and ΔPT-infected animals (Table 1). Despite high RV pressures, cardiac output was maintained in WT-infected infant mice at 7 dpi (Table 1).

DISCUSSION

Pertussis-associated PH is a major risk factor and potential cause of death in *B. pertussis*-infected infants [3]. In this work, we describe the first *B. pertussis* infection-induced model of PH. This platform will enable the study of molecular mechanisms potentiating *B. pertussis*-induced PH and the rational design and validation of PH-targeted therapeutics. Indeed, in the present work, this model was used to provide the first experimental evidence that PT promotes PH during *B. pertussis* infection.

Table 1. Right Heart Catheterization and Echocardiography

Variable	PBS (n = 11)	WT (n = 11)	*P* Value vs PBS	ΔPT (n = 6)	*P* Value vs PBS	*P* Value WT vs ΔPT
Body weight, g	6.31 (1)	4.95 (0.23)	.0002 ***	6.8 (0.17)	.341	<.0001 ****
Right heart catheterization						
Heart rate, bpm	454 (83)	469 (88)	.91	464 (70)	.97	.993
RVESP, mmHg	16.8 (2.9)	22.7 (4.4)	.003 **	15 (3.5)	.592	.001 **
RVEDP, mmHg	1.49 (0.66)	2.61 (1)	.02 *	2.39 (1.1)	.1379	.889
RV dP/dt max, mmHg/s	757 (190)	1209 (252)	<.0001 ****	669 (82)	.6727	<.0001 ****
RV dP/dt min, mmHg/s	−826 (200)	−1233 (481)	.021 *	−573 (89)	.308	.002 **
Right heart echocardiography						
Heart rate, bpm	399 (87)	400 (50)	.999	364 (77)	.618	.608
RVWs, mm	0.39 (0.07)	0.61 (0.14)	.0001 ***	0.46 (0.06)	.5	.018 *
RVWd, mm	0.28 (0.04)	0.48 (0.13)	<.0001 ****	0.33 (0.06)	.54	.005 **
AT, ms	22.7 (5.1)	15.1 (2.9)	.0005 ***	17.9 (3.7)	.067	.39
mPAP, mmHg	31.2 (6.2)	40.4 (3.5)	.0005 ***	37 (4.5)	.068	.387
PA, mm	0.91 (0.21)	0.97 (0.21)	.782	0.95 (0.13)	.92	.983
PA area, mm^2	0.69 (0.32)	0.76 (0.31)	.804	0.72 (0.21)	.969	.955
PA VTI, mm	28.2 (6.7)	34.1 (7.5)	.109	29.1 (4.1)	.961	.308
Stroke volume, μL	20.7 (13.3)	27.7 (15.1)	.435	20.8 (5.6)	>.999	.555
Cardiac output, mL/min	8.9 (6.6)	11.2 (6.9)	.657	7.3 (1.4)	.874	.444

Values are mean (SD). *P* value determined by 1-way ANOVA with Tukey multiple comparison test; $*P < .05$, $**P < .01$, $***P < .001$, $***P < .0001$.

Abbreviations: ANOVA, analysis of variance; AT, acceleration time; mPAP, mean PA pressure; PA, pulmonary artery; VTI, velocity time integral; PBS, phosphate-buffered saline; WT, pertussis toxn-expressing *B. pertussis;* ΔPT, pertussis toxin-deficient strain; RV, right ventricular; RV dP/dt max/min, maximum/minimum rate of RV pressure rise or fall; RVEDP, RV end-diastolic pressure; RVESP, RV end-systolic pressure; RVWd, RV free wall thickness at end-diastole; RVWs, RV free wall thickness at end-systole.

Here, we compared the impact of *B. pertussis* on the RV wall in infant and adult pertussis models and found a rapid, infection-induced RV remodeling in infant mice but not in adults. The small size of the infant mouse heart is a major limiting factor in the study of age-related cardiac responses. In 2018, a new mouse model of PH induced by respiratory syncytial virus was established. In that model, mice received a primary challenge at P5, were reinfected 4 weeks later and PH was then determined at this older age by echocardiology and RV catheterization [8]. To our knowledge, this is the first description of Fulton index and RV pressure in an infant mouse and the first use of Doppler echocardiogram to assess infection-induced cardiac remodeling in a P14 mouse. Typically, maladaptive RV changes are associated with altered right ventriculoarterial coupling, characterized by dilated RV with reduced stroke volume, altered systolic function, and increased filling pressures [4]. At 7 dpi, stroke volume was maintained in infected infant mice; however, changes in systolic function and filling pressures were detected. In PH, an increase in pulmonary vascular resistance leads to enhanced RV inotropy or contractility to maintain flow [11]. The rate of rise in intraventricular pressure (dP/dt) was used here as a surrogate for contractility and was markedly increased in *B. pertussis*-infected infant mice. PT expression by *B. pertussis* was required to induce enhanced contractility, indicating that PT promotes pulmonary resistance to initiate PH. RVESP was significantly greater in animals infected with a PT-expressing *B. pertussis* strain compared with those infected with ΔPT or sham inoculated, supporting a role for PT in increasing RV afterload. Whether PT increases pulmonary resistance by enhancing circulating white blood cell numbers (leukocytosis) or promoting pulmonary vascular remodeling remains to be determined. PT, an inhibitor of G protein-coupled receptors, may also be acting directly on cardiomyocytes to cause cardiac dysfunction. Indeed, PT injected into rats ablated the effect of a negative inotropic and chronotropic agent on the heart, while positive inotropic effects were increased with toxin treatment [12]. In addition, our group has evidence that PT-mediated regulation of angiotensin II signaling correlates with severe outcomes in the infant pertussis model (K. S. unpublished). Increased filling pressure (RVEDP) was observed with both WT and ΔPT infection, though this was only significant for WT. RVEDP is more a function of pericardial and intrathoracic pressure and not a change in RV distending pressure (intraventricular pressure minus pericardial pressure) [4]. At 7 dpi, ΔPT-infected (but not WT-infected) infant mice display significant pulmonary inflammation [7]. Therefore, increased RVEDP with ΔPT infection might represent increased juxtacardiac intrathoracic pressure as a result of lung inflammation, but this will require further examination.

The mechanisms promoting severe pertussis in infancy are poorly defined. It is known that immune responses to pathogens are age related, with infants adopting a disease tolerance defense strategy rather than a disease resistance approach [13]. In our earlier work, we found that *B. pertussis* displayed enhanced lung colonization and systemic dissemination in infant mice as compared with adult mouse infection [7]. The identification of *B. pertussis* in humans is routinely performed on samples recovered only from the respiratory tract; however, in a study reviewing 6 fatal

pertussis cases in infants, *B. pertussis* was detected by polymerase chain reaction (PCR) in blood samples from 2 of the 6 patients [14]. In infants, such bacterial outgrowth likely correlates with increased quantities of PT and, with bacterial dissemination, PT intoxication may occur in organs otherwise not affected in older individuals. Hence, PT-mediated pathologies may be exacerbated by the infant immune response aiming to limit inflammatory damage and energy consumption rather than achieving bacterial killing. Further studies are required to determine whether the infant pulmonary system is primed for enhanced structural and functional cardiac changes in response to increased pulmonary resistance as compared with the adult system. Indeed, it is known that hypoxemia can maintain the proliferative window of neonatal cardiomyocytes, while adult cardiomyocytes are resistant to reentering the cell cycle [15]. Future experiments will investigate the impact of host age on cardiac adaptations to increased pulmonary resistance.

PT expression by *B. pertussis* is required for infection-induced infant death [7] and, in this work, PT promoted features of PH. While cardiac arrest and failure are described in infant pertussis, whether PH is the primary cause of *B. pertussis*-induced death is unknown. The dramatic PT-dependent increase in RV contractility to overcome afterload and maintain cardiac output described here would require significant amounts of energy. Right heart coronary perfusion is decoupled from afterload and hence this high metabolic demand leads to RV failure [4], while the increased energy requirements may also further impair immune function and cause multiple organ failure [13]. The model described in this work will enable us to start examining these hypotheses and facilitate the testing of PH-targeted treatment options.

Supplementary Data

Supplementary materials are available at *The Journal of Infectious Diseases* online. Consisting of data provided by the authors to benefit the reader, the posted materials are not copyedited and are the sole responsibility of the authors, so questions or comments should be addressed to the corresponding author.

Notes

Financial support. This work was supported by the National Institutes of Health National Institute of Allergy and Infectious Diseases (grant numbers AI151485 to K. S. and AI141372 to N. C.).

Potential conflicts of interest. All authors: No reported conflicts of interest. All authors have submitted the ICMJE Form for Disclosure of Potential Conflicts of Interest. Conflicts that the editors consider relevant to the content of the manuscript have been disclosed.

Presented in part: Biology of Acute Respiratory Infection Gordon Research Conference, March 2018, Venture, CA; 12th International Bordetella Symposium, April 2019, Brussels, Belgium; and American Society for Microbiology Annual Meeting, June 2019, San Francisco, CA.

References

1. Yeung KHT, Duclos P, Nelson EAS, Hutubessy RCW. An update of the global burden of pertussis in children younger than 5 years: a modelling study. Lancet Infect Dis **2017**; 17:974–80.
2. McEniery JA, Delbridge RG, Reith DM. Infant pertussis deaths and the management of cardiovascular compromise. J Paediatr Child Health **2004**; 40:230–2.
3. Winter K, Zipprich J, Harriman K, et al. Risk factors associated with infant deaths from pertussis: a case-control study. Clin Infect Dis **2015**; 61:1099–106.
4. Pinsky MR. The right ventricle: interaction with the pulmonary circulation. Crit Care **2016**; 20:266.
5. Halasa NB, Barr FE, Johnson JE, Edwards KM. Fatal pulmonary hypertension associated with pertussis in infants: does extracorporeal membrane oxygenation have a role? Pediatrics **2003**; 112:1274–8.
6. Burr JS, Jenkins TL, Harrison R, et al. The collaborative pediatric critical care research network critical pertussis study: collaborative research in pediatric critical care medicine. Pediatr Crit Care Med **2011**; 12:387–92.
7. Scanlon KM, Snyder YG, Skerry C, Carbonetti NH. Fatal pertussis in the neonatal mouse model is associated with pertussis toxin-mediated pathology beyond the airways. Infect Immun **2017**; 85:e00355–17.
8. Kimura D, Saravia J, Jaligama S, et al. New mouse model of pulmonary hypertension induced by respiratory syncytial virus bronchiolitis. Am J Physiol Heart Circ Physiol **2018**; 315:H581–9.
9. Marra AM, Benjamin N, Ferrara F, et al. Reference ranges and determinants of right ventricle outflow tract acceleration time in healthy adults by two-dimensional echocardiography. Int J Cardiovasc Imaging **2017**; 33:219–26.
10. Ameloot K, Palmers PJ, Vande Bruaene A, et al. Clinical value of echocardiographic Doppler-derived right ventricular dP/dt in patients with pulmonary arterial hypertension. Eur Heart J Cardiovasc Imaging **2014**; 15:1411–9.
11. Vonk Noordegraaf A, Westerhof BE, Westerhof N. The relationship between the right ventricle and its load in pulmonary hypertension. J Am Coll Cardiol **2017**; 69:236–43.
12. Tucek S, Dolezal V, Folbergrová J, Hynie S, Kolár F, Ostádal B. Pertussis toxin inhibits negative inotropic and negative chronotropic muscarinic cholinergic effects on the heart. Pflugers Arch **1987**; 408:167–72.
13. Harbeson D, Ben-Othman R, Amenyogbe N, Kollmann TR. Outgrowing the immaturity myth: the cost of defending from neonatal infectious disease. Front Immunol **2018**; 9:1077.

14. Carloni I, Ricci S, Azzari C, Galletti S, Faldella G, de Benedictis FM. Fatal pertussis in infancy, Italy. J Infect **2017**; 75:186–9.

15. Puente BN, Kimura W, Muralidhar SA, et al. The oxygen-rich postnatal environment induces cardiomyocyte cell-cycle arrest through DNA damage response. Cell **2014**; 157:565–79.